J. Chem. Soc., Faraday Trans. 2, 1987, **83**, 747–757

Dynamical Scattering and the Quantification of Electron Energy-loss Spectra of Solids

Richard D. Brydson, John M. Thomas*† and Brian G. Williams

Department of Physical Chemistry, University of Cambridge, Lensfield Road, Cambridge CB2 1EP

An important application of electron energy-loss spectroscopy (EELS) carried out in the electron microscope is to the elemental analysis of microscopic samples which may be as small as 1 nm in linear dimension, *i.e.* in samples of only 10^{-20} g. This technique is particularly important for the study of the first row elements of the periodic table which are not easily investigated using the alternative technique of X-ray emission spectroscopy (XRE). Until recently it was thought that uncertainties of some 10% were associated with the detection limit for light elements and for the accuracy with which the concentration of light elements present in the sample could be measured. This limit stems in part from the inaccuracies inherent in the random statistics of the counting process and in part from systematic errors in the calculation of the relevant cross-sections and corrections. However, the improved understanding of the various systematic errors and corrections as well as recent developments in parallel detection means that it should now be possible to carry out chemical analyses with an accuracy of the order of 1% or better. We examine the effect of Bragg scattering, which in electron microscopy must be trated in the dynamical scattering limit, on the accuracy of elemental analysis using EELS. Neglect of this effect may lead to errors of up to 20% in the chemical analysis. The theory of such multiple scattering is outlined and three representative samples are studied: boron nitride, nickel oxide and silicon. These examples permit us to examine the effect of Bragg scattering on estimates of the relative amounts of two elements as well as on estimates of the absolute amounts of a single element.

When equipped with the appropriate detectors an electron microscope constitutes one of the most powerful and sensitive instruments for chemical analysis: minimum detectable limits are of the order of 10^{-20} g. There are[1] two principle ways of effecting quantitative elemental analysis by electron microscopy: recording the characteristic X-rays emitted (X-ray emission spectroscopy, XRE) as a result of bombardment of the sample by the primary electron beam, or recording the characteristic losses in energy suffered by the primary beam as a result of core-electron excitation during the irradiation of the specimen (electron energy loss spectroscopy EELS). Other methods of chemical analysis,[2,3] such as plasmon spectroscopy, are possible but these are not generally applicable. XRE is best suited for the analysis of elements of atomic number $Z > 10$, in view of the fact that the soft X-rays emitted from elements with $Z < 10$ are readily absorbed thereby yielding greater experimental uncertainties. With the advent of window-less X-ray detectors this difficulty is minimized; however, solid-state detectors are intrinsically incapable of very high energy resolution, so that it is doubtful whether information pertaining to chemical shifts arising from environmentally distinct atoms will ever be achieved by methods based on XRE.

† Present address: Davy-Faraday Laboratories, The Royal Institution, 21 Albermarle Street, London W1X 4BS.

With EELS, however, not only is it an intrinsically superior technique for the detection of light elements such as carbon, nitrogen and oxygen, it is also capable, in view of the resolution already attainable (*ca.* 1 eV) with electron spectrometers, of yielding information both on chemical shifts arising from atoms in different environments and also on the oxidation states of certain, notably transition metal, elements. In the first instance, however, the aim is to improve the precision of elemental analysis by EELS. The prospects of doing so are promising especially when parallel recording and other improvements are fully developed.

There are, however, a number of important strategic issues which need first to be considered before EELS becomes a routine analytical technique. These devolve upon the way in which the data are recorded and, in turn, relate to the various corrupting influences of subsidiary electronic processes that take place before or after the energy-loss by core-electron excitation. In this paper we examine the effect of dynamical scattering on the quantification of EELS data.

Background Theory

When high-energy electrons traverse a thin film they may lose energy in a number of different ways. In particular, if the energy transferred in the scattering process exceeds the binding energy of the core electrons in the sample, it is possible to excite these electrons into an empty state at or above the Fermi energy. The energy-loss spectrum then exhibits steps at energies corresponding to the electron binding energies so that from the positions of these steps and a table of atomic energy levels[4] a qualitative analysis of the sample can be made. If, in addition, the cross-section for exciting each edge is known, it is possible to quantify the analysis and, to this end, Egerton[5] has written, and made generally available, two computer programs known as SIGMAK and SIGMAL, which calculate the cross-sections for hydrogenic wavefunctions. These experiments entail the use of primary beams of between *ca.* 50 and 200 keV and a magnetic prism spectrometer with an energy resolution of *ca.* 1 eV.

If σ is the cross-section for exciting an edge, and I_i and I_s are the intensities in the incident beam and in the core edge, respectively, then the corresponding number of atoms per unit area in the sample, N, is given by

$$N = (1/\sigma)(I_s/I_i) \quad (1)$$

so that the determination of the elemental composition of a sample is, in principle, quite straightforward.

In practice a number of systematic corrections must be considered, in addition to allowing for the inaccuracies introduced by the counting statistics. Some of the more important corrections are as follows: (i) The cross-section calculations are carried out using free-atom wavefunctions, and these will not reproduce the ELNES (electron-loss near-edge structure) features which are observed close to the edges in measurements on solids. However, experience shows that solid-state effects tend to redistribute the signal close to the edge, so that if the edge intensity is measured over a window of 50 eV or more, the calculated cross-sections are reasonably accurate. The choice of the energy window over which to determine the intensity in the edge is clearly important. (ii) The angular dependence of the cross-section for exciting a particular edge varies between one edge and another, and the calculated cross-section must make allowance for the acceptance angle of the spectrometer and the convergence angle of the incident beam. (iii) Multiple inelastic scattering can be important, the dominant effect being edge-plasmon scattering in which the excitation of an edge is preceded or followed by the excitation of a plasmon,[6] and when the sample thickness is equal to the plasmon mean free path (typically *ca.* 1000 Å) multiple inelastic scattering may introduce errors of *ca.* 15% in the elemental analysis. (iv) The statistical accuracy with which the area under

an edge can be determined depends on the total number of counts which are collected but also on the signal to background ratio. The dominant inelastic scattering process involves plasmon excitation and the edges sit on the tail of the plasmon lines, so that the signal-to-noise ratio improves significantly as the sample thickness decreases below the plasmon mean free path. In addition, the angular distribution for inelastic scattering events varies inversely with the characteristic energy-loss so that the low-energy plasmon excitations are spread out over a wide range of angles while the core-excitations are more concentrated in the forward direction. Consequently, a small collection angle will provide the best signal-to-background ratio but will also reduce the total number of counts which are collected.

As experimental techniques are improved and more refined treatment of the data is carried out, the accuracy of elemental analysis using EELS is improving from *ca.* 10% down to *ca.* 1%. However, there is one important effect which has received relatively little attention, and this is multiple scattering in which a Bragg scattering event is followed by an inelastic scattering event. In this paper the consequences of such combined events for elemental analysis using EELS is examined in detail.

Elastic Scattering

To assess the effects of Bragg scattering on elemental analysis using EELS, Egerton[7] considered the probability that an electron which has been scattered elastically through a non-zero angle will then be scattered into the collection aperture as a result of the excitation of a core electron. Using essentially kinematical arguments he concluded that, for amorphous samples, elastic–inelastic scattering events will affect the analysis by less than 1%, but that for crystalline samples significant errors will be introduced if there is a strongly excited Bragg beam just inside or just outside the collection aperture. A collection aperture for which the semi-angle α is less than half the smallest Bragg angle is therefore recommended. Since at an incident beam energy of 100 keV the smallest Bragg angle is typically *ca.* 10 mrad, the recommended value of α is *ca.* 5 mrad.

Bourdillon and Stobbs[8] have also considered this problem. They used a semi-empirical distribution for the elastic scattering to obtain the cross-section for elastic–inelastic scattering into the collection aperture. To circumvent the calculation of mean free paths and specimen thickness, they measured the intensity of elastic scattering as a function of angle using a tilted and conically scanned incident beam. They concluded that the effects of elastic scattering are most noticeable for small collection apertures and thick samples, and that when applied to the ratio of two elements the magnitude of the correction, typically *ca.* 5%, also depend on the energy separation of the core thresholds. In neither of these two studies has dynamical scattering been included explicitly. It is possible, however, to cope explicitly with the problems arising from dynamical scattering; this is done in simulation of high-resolution images as a function of thickness and defocus.[9–11] Such procedures are central to all aspects of electron microscopy. In a previous paper[12] we studied the effect of dynamical scattering on the determination of Compton profiles in the electron microscope. Using a multi-slice program, developed by Uppal for the simulation of lattice images, to calculate the intensity in the low-order Bragg beams as a function of the sample thickness, we were able to treat each Bragg beam as a source of Compton scattering and hence to investigate the effect of Bragg–Compton multiple scattering events on Comptom profile measurements. In this paper we proceed to investigate the effect of Bragg core-edge scattering on elemental analysis in the same way.

The angular distribution of the cross-section σ per unit solid angle Ω, for inner-shell scattering may be obtained by treating the scattering centre as a screened Coulomb potential,[13] so that

$$\mathrm{d}\sigma/\mathrm{d}\Omega \propto 1/(\theta^2 + \theta_E^2) \qquad (2)$$

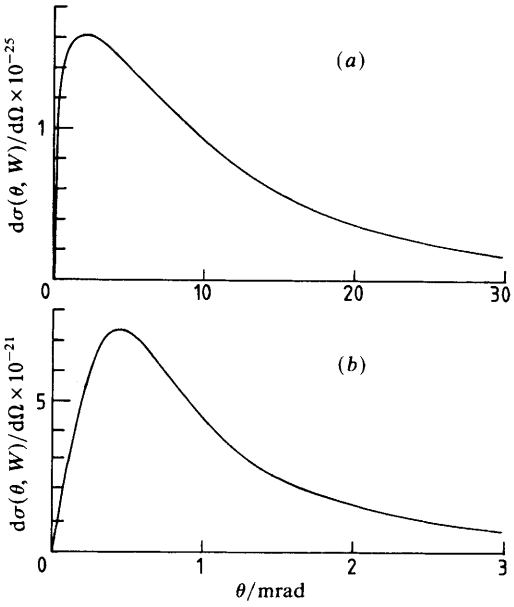

Fig. 1. The cross-section per unit solid angle for scattering through an angle θ in an energy window 100 eV above the silicon K-edge (a) and the silicon L-edge (b).

where θ is the scattering angle, $\theta_E = \Delta E/2E_i$ with ΔE the energy loss for the core excitation under consideration and E_i the energy of the incident beam. Eqn (2) shows that the angular distribution of the inelastic scattering is essentially Lorentzian, but to obtain a more accurate form for the angular dependence of inner-shell scattering we have used Egerton's SIGMA programs to evaluate $\sigma(\alpha, W)$, the cross-section for scattering into a central aperture of semi-angle α in an energy window W above the edge at ΔE:

$$\sigma(\alpha, W) = 2\pi \int_{\Delta E}^{\Delta E + W} \int_0^{\alpha} (d^2\sigma/d\Omega\, dE)\theta\, d\theta\, dE. \tag{3}$$

The cross-section per unit solid angle for scattering through an angle α in an energy window W, is then

$$d\sigma(\theta, W)/d\Omega = (1/2\pi\alpha)[d\sigma(\alpha, W)/d\alpha]|_{\alpha=\theta}. \tag{4}$$

Fig. 1 shows $d\sigma(\theta, W)/d\Omega$ as a function of angle for the silicon K- and L-edges at an incident energy of 100 keV and with an energy window of 100 eV. The L-shell excitation, for which ΔE is equal to 99 eV, has a very compact angular distribution, the value of θ_E in eqn (2) being 0.5 mrad, the peak occurring at $\theta_p = 0.5$ mrad, with the curve falling back to one half of its peak value at $\theta_h = 1.2$ mrad. The K-shell excitation on the other hand, for which $\Delta E = 1839$ eV, has a much wider angular distribution with $\theta_E = 9$ mrad, $\theta_p = 2$ mrad and $\theta_h = 11$ mrad. Note also that the initial rise is relatively sharp for the K-shell as compared to the L-shell.

Estimating the contribution to the core edge for a given shell in a given element is now straightforward. The multi-slice program is run for the sample under consideration, and the intensity in each of the significant Bragg beams, averaged over the thickness of the sample, is obtained. (The slice thickness is taken to be half of the unit cell, which our previous experience has shown to be sufficiently small.[12]) Each of these beams is then treated as a source of core-edge excitation, and the probability of scattering from a given Bragg beam, back into the central aperture, is calculated by integrating functions

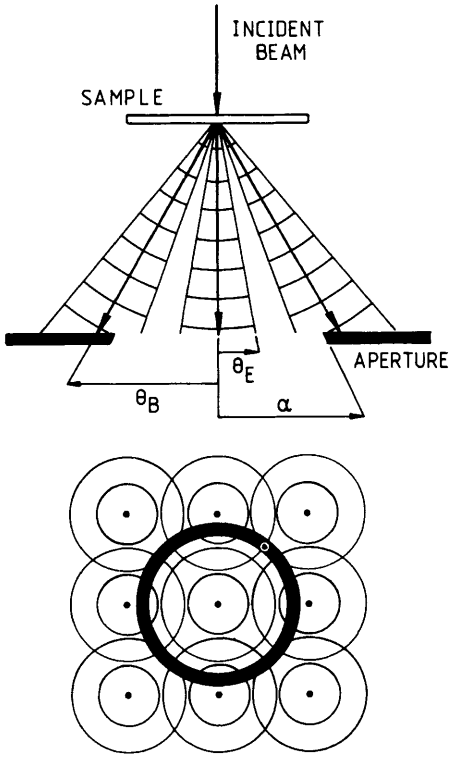

Fig. 2. Schematic diagram showing two Bragg beams at an angle θ_B to the straight-through beam, with the inelastic scattering spread out over cones of semi-angle θ_E about the straight-through and the Bragg beams, being intercepted by the collection aperture with semi-angle α. The lower part of the figure shows the straight-through beam and eight Bragg beams in the diffraction plane, each of which is surrounded by the inelastic scattering from two edges. The annulus (heavy back circle) represents the collection aperture. The area outside the annulus is naturally blocked off in the experiment.

such as those illustrated in fig. 1 over a circular aperture whose centre lies at the Bragg angle under consideration. This is illustrated in fig. 2, where two Bragg beams are shown at an angle of θ_B to the unscattered beam, and the inelastic scattering occurs in a cone of semi-angle θ_E about each of these. The collection aperture of semi-angle α is shown intercepting all of the central beam and a part of the inelastic scattering from the two Bragg beams. In the lower part of fig. 2 the same situation is illustrated, but now in the diffraction plane. Eight Bragg beams are shown, each one surrounded by two circles representing the angular range over which each of two different edges produces significant scattering, and the thick circle represents the collection aperture. It is clear that the precise intensity one observes in each edge will in general depend on the symmetry of the diffraction pattern, the Bragg angles, the characteristic angles for the edges under consideration and the diameter of the aperture in a rather complex way.

Ideally one should also include the inverse process in which an edge excitation is followed by a Bragg diffraction. The contribution from such processes is more difficult to calculate. After exciting a core electron, the scattered electron will spread out as a spherical wave. This would then have to be expanded in plane waves and for each plane wave a dynamical scattering calculation would be needed to determine the extent to which these electrons excite further Bragg beams. Electrons which have lost very little energy are highly focussed in the forward direction so that they excite the same

Laue zone of spots, as does the unscattered beam, and the effect is to produce slightly broadened spots.[14,15] For edges above a few hundred electron volts, on the other hand, the angular spread in the scattered beam may exceed the angular separation of the Bragg beams, giving rise to Kossel- (or Kikuchi-) like bands. It seems reasonable to argue that these two effects, Bragg scattering followed by an edge excitation or *vice versa*, should be of comparable magnitude. Thus, if conditions can be found in which the former is reduced to manageable proportions the latter effect should be equally small. We hope to investigate these effects experimentally in the future, and this should provide a test of our present calculations and also help to elucidate the importance of the inverse process.

Results

The samples chosen for the simulations were cubic boron nitride, nickel oxide and silicon, all of which have cubic symmetry. Boron nitride was chosen because EELS is at its best when studying edges of the elements beryllium to oxygen and the edges are quite close together in energy. Nickel oxide was chosen as this provides two edges, the nickel L-edge and the oxygen K-edge, which are typical of the edges on which chemical analysis is routinely done. Silicon was chosen because the K- and L-edges are well separated in energy, so that the effects under consideration should be large, and also because this is an ideal test sample for experimentation: the ratio of the amount of silicon calculated from the K- and L-shells should be exactly 1. Initially we consider the accuracy with which the ratio of the concentrations of two elements can be estimated, and we then consider the problems associated with absolute quantification of the elemental analysis.

For each simulation the total intensity scattered inelastically into the aperture in a given energy window from all of the Bragg beams is calculated, and the apparent elemental ratio is then determined after allowing for the energy window and the aperture as though there were no multiple scattering. The deviations from 1 therefore represent the error in the elemental ratio which arises from Bragg scattering.

Boron Nitride

Fig. 3 shows the results obtained for a boron nitride sample 100 Å thick with a 100 keV beam incident on the crystal in the (100) direction. The apparent ratio deviates from 1 by $<2\%$ for all angles, and the greatest deviation is at the first Bragg spot. In this simulation the intensity in the straight-through beam is $>90\%$ for all thicknesses up to 100 Å so that dynamical scattering effects are relatively unimportant and the angular dependence can be explained as follows. The binding energies of the boron and nitrogen K-edges are 188 and 402 eV, respectively, the corresponding θ_E values being 0.9 and 2.0 mrad. For small collection angles the contribution to the edge intensity from the first Bragg spot will be greater for nitrogen than for boron, as the nitrogen signal is spread out over a wider angular range, and the ratio will decrease further as the collection angle is increased. Once the first Bragg spot is contained within the aperture, however, the narrow angular spread of the boron edge will cause the boron contribution to increase more rapidly than the nitrogen contribution, so that the apparent ratio of boron to nitrogen increases, the turning point being close to the position of the (020) beam. By the time the (022) beam is included in the aperture the apparent ratio of boron to nitrogen becomes greater than 1 and then above 22 mrad it converges back to 1.

Nickel Oxide

The oxygen K-edge is 532 eV and the nickel L-edge is at 860 eV (L_2 at 855 eV, L_3 at 873 eV), so that the characteristic angles are 2.7 and 4.3 mrad, 2 to 3 times as great as

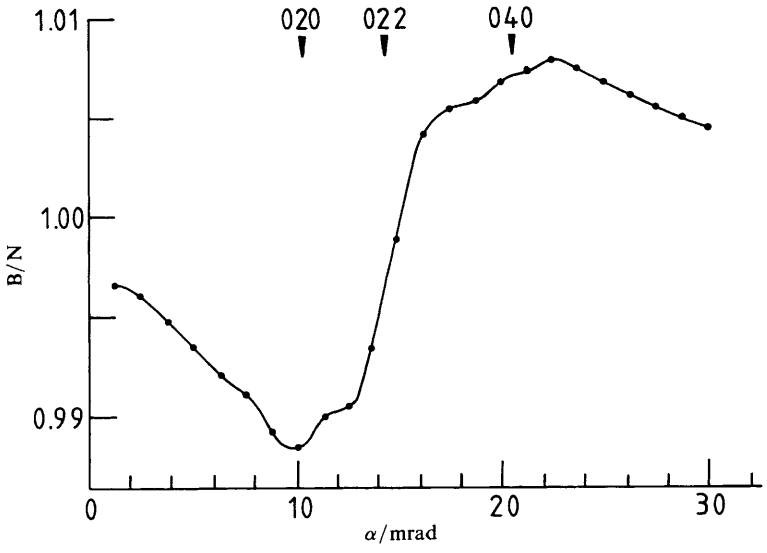

Fig. 3. The apparent ratio of boron to nitrogen as a function of the collection semi-angle α. The arrows mark the positions of the most intense Bragg beams.

in boron nitride. Furthermore dynamical scattering effects are more important, the intensity in the straight-through beam falling to 70% of the intensity in the incident beam after 100 Å.

Fig. 4 shows the apparent ratio of oxygen to nickel as a function of collection semi-angle, and at very small angles it deviates from 1 by 5.5%. The angular dependence of the apparent ratio of oxygen to nickel shows more structure, with the contributions from neighbouring beams overlapping in a more complex way. To interpret the structure observed in fig. 4 we consider eqn (1) in more detail. The ratio of oxygen to nickel is given by

$$R = (\sigma_{Ni}/\sigma_O)(I_O/I_{Ni}) \tag{5}$$

where the intensity in the oxygen edge, for example, is the intensity from the straight-through beam, I_O^S plus the intensity from all of the Bragg beams, I_O^B, so that

$$I_O = I_O^S + I_O^B. \tag{6}$$

Since the calculated cross-sections allow for the energy window and the collection semi-angle

$$(\sigma_{Ni}/\sigma_O)(I_O^S/I_{Ni}^S) = 1 \tag{7}$$

so that

$$R = (1 + I_O^B/I_O^S)/(1 + I_{Ni}^B/I_{Ni}^S). \tag{8}$$

We can now explain the structure observed in the nickel oxide edge. Below 2 mrad I_{Ni}^S is very small because of the relatively slow rise at small angles. As a result the apparent ratio is small but increases rapidly as the collection angle increases up to *ca.* 4 mrad. At 4 mrad the Bragg-edge contribution from nickel, I_{Ni}^B, begins to contribute and the apparent ratio decreases slightly. As the aperture semi-angle is increased further successive contributions from the nickel and oxygen edges are included and the curve converges in an oscillatory fashion.

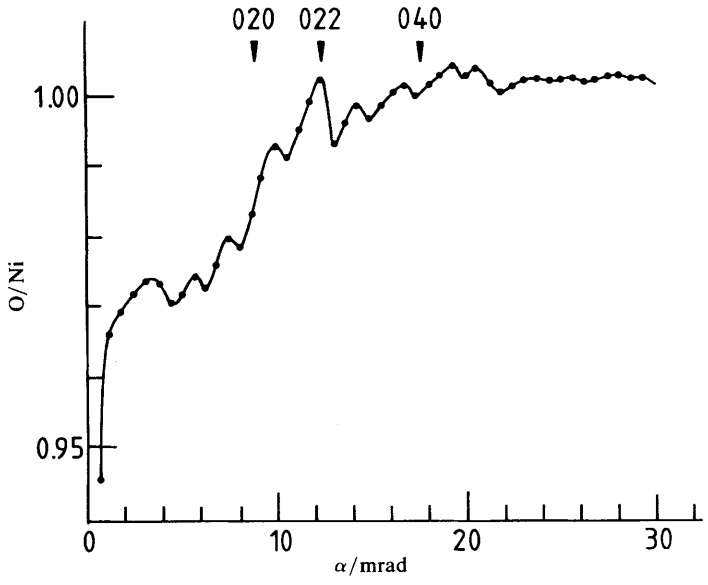

Fig. 4. The apparent ratio of oxygen to nickel as a function of the collection semi-angle α. The arrows mark the positions of the most intense Bragg beams.

Silicon

Silicon represents an extreme case: there are two edges which can be used to test the model calculations, the *L*-edge at 99 eV and the *K*-edge at 1839 eV. Since the edges are well separated in energy the effect of the dynamical scattering should be large and of course the ratio of the amount of silicon present, determined from the two edges, must be exactly 1.

Fig. 5 shows a plot of the apparent ratio of silicon to silicon for a sample 136 Å thick. As above, a 100 keV incident beam is taken to be incident on the sample in the (100) direction and the energy window is 100 eV. The θ_E values for the two edges are now 0.75 and 9.5 mrad, so that the first is much less than the spacing between the Bragg spots while the second is almost equal to the spacing between the Bragg spots. The multi-slice calculation showed that there is strong dynamical scattering, the intensity in the straight-through beam falling to *ca.* 30% of the initial value after 100 Å.

The apparent ratio now differs from 1 by as much as 30% at small collection angles, and the general behaviour of the curve can again be explained in terms of the characteristic angles and the positions of the Bragg spots. The initial increase in the curve at very small angles arises from the slow convergence to zero for the *L*-edge at small angles as in the case of nickel oxide. The curve then remains fairly constant but significantly below 1 because of the greater contribution from the *K*-shell. The *L*-shell scattering is very tightly concentrated around the Bragg spots in each case, so that once the spots enter the aperture the apparent ratio increases rapidly and beyond *ca.* 25 Å the correction is less than a few percent.

Absolute Quantification

In the discussion so far we have considered only the effect of dynamical scattering on the estimation of the ratios of the amounts of two elements which are present in the sample, and indeed this is often all that is required. However, there are situations in

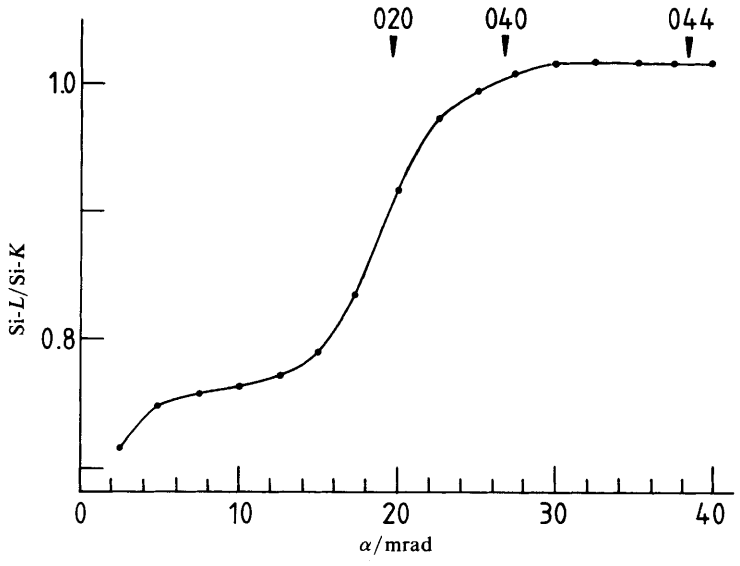

Fig. 5. The apparent ratio of silicon K-shell to L-shell scattering as a function of the collection semi-angle α. The arrows mark the positions of the most intense Bragg beams.

which one would like to estimate the amount of each element present on an absolute basis, and this is a more difficult task.

In addition to the problems encountered in the ratio analysis, we now have the problem of deciding on the correct normalization criterion. Suppose we could ignore multiple Bragg-edge scattering, so that once a Bragg beam has been excited it will never scatter back into the spectrometer aperture, as would apply in the case of very small collection apertures and low-energy edges. The correct procedure would then be to divide the intensity in the edge by the average intensity in the straight-through beam as it traverses the sample. Allowing for the scattering cross-section would then give the correct, absolute elemental analysis. In practice, however, we can only measure the intensity in the incident beam and the intensity in the straight-through beam as it emerges from the sample. Under so-called kinematical conditions (when only one scattering event need be considered) one could extrapolate between these two values to determine the appropriate intensity to use in the calculation. Under dynamical scattering conditions, however, the intensity in the straight-through beam may oscillate with a period of only 200 Å (in the case of silicon[12]), and errors of up to 20% can easily be introduced.

This is illustrated for silicon in fig. 6(a), which shows the amount of silicon (normalized to the correct value) which one obtains if the K-edge intensity is measured with respect to the intensity in the incident beam, and in fig. 6(b), which shows the same quantity but with the edge intensity normalized to the intensity in the elastic line, *i.e.* the intensity in all of the Bragg beams which are included in the aperture.

Below 10 mrad the curves are essentially the same apart from the normalization. The intensity in the incident beam represents too large a number and the apparent amount is <1, while the intensity in the straight-through beam at the bottom of the crystal is too small and the apparent amount is >1. As the semi-angle of the collection aperture is increased, more of the Bragg-edge scattering is included and the apparent amount of silicon increases. With the first method of normalization the curve converges smoothly to 1 as more and more Bragg beams enter the aperture. With the second method of normalization, however, each time a Bragg beam enters the aperture, the

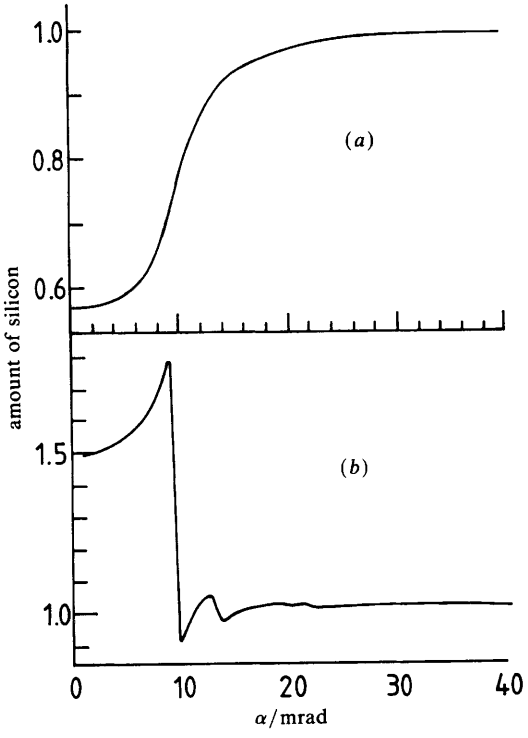

Fig. 6. The apparent amount of silicon (normalized to the correct value) obtained if the dynamical scattering effects are not accounted for. In (*a*) the *K*-edge intensity is measured with respect to the intensity in the incident beam and in (*b*) the edge intensity is normalized to the intensity in the elastic line, that is to say the intensity in all of the Bragg beams which are included in the aperture.

elastic line undergoes a dramatic increase and the apparent amount of the element drops discontinuously. In practice it will clearly be advisable to measure both and, in the absence of dynamical scattering calculations, to use their mean in the normalization.

Conclusions

This paper represents the first attempt to investigate the effects of dynamical scattering on quantitative elemental analysis using EELS. The nature of these calculations is such that they include any order of dynamical scattering followed by a single inelastic scattering; they do not address the related problem in which inelastic scattering is followed by Bragg scattering. We intend in future work to investigate the predictions made in this paper experimentally but are already able to draw a number of conclusions.

(i) It is important to perform ratio-analysis using edges which are as close together in energy as possible, within the limits imposed by the need to have a window of *ca.* 50 eV over which to determine the edge intensity.

(ii) Some workers have suggested that the optimal collection semi-angle for ratio analysis is *ca.* 5 mrad, while others recommend using much larger collection angles of *ca.* 100 mrad. While it is true that very large collection angles will minimise the problems discussed in this paper the signal-to-noise ratio will then be considerably worse and the quality of the data will suffer accordingly. As a result of this study we suggest that a collection semi-angle of 15–20 mrads provides the optimal compromise between the

need to minimise systematic errors arising from multiple scattering while maintaining a reasonable signal-to-background ratio. With such collection angles the nearest and possibly the second-nearest Bragg spots will be included in the collection aperture.

(iii) It is clear from this study that dynamical scattering may introduce significant systematic errors, and since, in electron microscopy, the relative intensities of the various Bragg beams depends critically on the precise orientation of the sample with respect to the incident beam, it will always be advantageous to orient the sample in such a way that as few Bragg beams as possible are excited.

We thank the S.E.R.C. for a research grant (to J.M.T.) and a quota studentship (to R.D.B.) and the Royal Society for a Senior Fellowship (to B.G.W.).

References

1 M. Beer, R. W. Carpenter, L. Eyring, C. E. Lyman and J. M. Thomas, *Chem. Eng. News*, 1981, **59**, 40.
2 J. M. Thomas, B. G. Williams and T. G. Sparrow, *Acc. Chem. Res.*, 1985, **18**, 324.
3 J. M. Thomas, T. G. Sparrow, M. K. Uppal and B. G. Williams, *Philos. Trans. R. Soc. London, Ser. A*, 1985, **318**, 259.
4 *Handbook of Chemistry and Physics*, ed. R. C. Weast (CRC Press, Cleveland, 55th edn, 1974).
5 R. F. Egerton, *Ultramicroscopy*, 1978, **3**, 243.
6 R. F. Egerton, *Ultramicroscopy*, 1981, **6**, 297.
7 R. F. Egerton, *Ultramicroscopy*, 1981, **6**, 243.
8 A. J. Bourdillon and W. M. Stobbs, *Ultramicroscopy*, 1981, **17**, 147.
9 D. A. Jefferson, G. R. Millward and J. M. Thomas, *Acta Crystallogr., Sect. A*, 1976, **32**, 823.
10 J. M. Thomas, *Ultramicroscopy*, 1982, **7**, 8.
11 D. A. Jefferson, *ACS Symp. Ser.*, 1985, **279**, 183.
12 B. G. Williams, M. K. Uppal and R. D. Brydson, *Proc. R. Soc. London*, 1987, in press.
13 C. Colliex, *Advances in Optical and Electron Microscopy*, ed. V. E. Cosslett (Academic Press, London, 1984).
14 R. F. Egerton, *Electron Energy Loss Spectroscopy* (Plenum Press, New York, 1986), p. 344.
15 J. M. Thomas, *ACS Symp. Ser.* 1983, **211**, 445.

Paper 6/1883; *Received* 22*nd September*, 1986